From Nonlinear System Analysis and Synthesis: Vol. 2 - Techniques and Applications , published by the American Society of Mechanical Engineers, 1980.

CHAPTER 9

APPLICATIONS OF A GENERAL LIMIT CYCLE ANALYSIS METHOD FOR MULTIVARIABLE SYSTEMS

James H. Taylor
General Electric Corporate
Research and Development
Bldg. 5 Room 233
Schenectady, New York 12345

Abstract. Using sinusoidal-input describing functions (SIDF's) is a well-known approach for studying limit cycles in nonlinear systems with one dominant nonlinearity [1,2]. In recent years, a number of extensions of the SIDF method have been developed to permit the analysis of systems containing more than one nonlinearity. In many cases, the nonlinear system models that can be treated by such extensions have been quite restrictive (limited to a few nonlinearities, or to certain specific configurations; cf. [2]). Furthermore, some results involved only conservative conditions for limit cycle avoidance, rather than actual limit cycle conditions. The technique described in this chapter and in [3] removes all constraints: Systems described by a general state vector differential equation, with any number of nonlinearities, may be analyzed. In addition, the nonlinearities may be multi-input, and bias effects can be treated.

The general SIDF approach was probably first fully developed and applied in [4]. It has also been applied to determine limit cycle conditions for rail vehicles; references for this work may be found in [3]. Its power and use are illustrated here by application to a second-order differential equation derived from a two-mode panel flutter model [5] and to a highly nonlinear model of a tactical aircraft in a medium-angle-of-attack flight regime [6,7]. Some problems associated with direct simulation (especially "obscuring modes" and the initial condition problem) are also discussed.

1. INTRODUCTION

The study of limit cycle (LC) conditions in nonlinear systems is a problem of considerable interest in engineering. An approach to LC analysis that has gained widespread acceptance is the frequency domain/sinusoidal-input describing function (SIDF) method [1,2]. This technique, as it was first developed for systems with

a single nonlinearity, involved formulating the system in the form

$$\dot{\underline{x}} = \underline{\bar{F}}\,\underline{x} + \underline{g}\mu$$
$$\sigma = \underline{h}^T\underline{x} \qquad (1)$$
$$\mu = \upsilon(t) - \phi(\sigma)$$

where $\underline{x}$ is an n-dimensional state vector. The first two relations describe a linear dynamic subsystem with input μ and output σ; the subsystem input is then given to be the external input signal $\upsilon(t)$ minus a nonlinear function of σ. There is thus one single-input/single-output (SISO) nonlinearity, $\phi(\sigma)$, and linear dynamics of arbitrary order that may be represented by the SISO transfer function (in Laplace transform notation) $W(s) = \underline{h}^T(s\underline{\bar{I}}-\underline{\bar{F}})^{-1}\,\underline{g}$. This system description is a modern control theoretic reformulation of the more conventional "linear plant in the forward path with a nonlinearity in the feedback path" [1,2], depicted in Fig. 1.

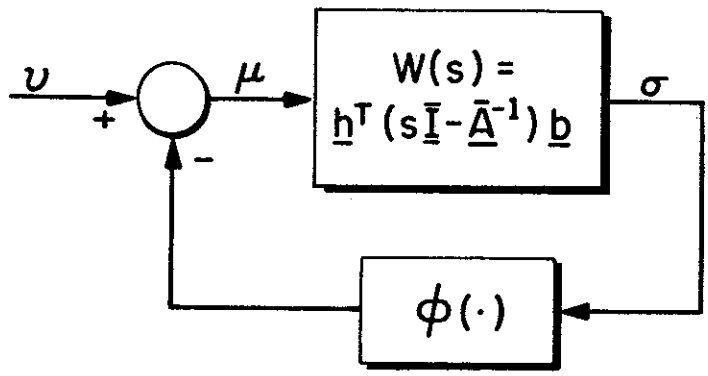

Fig. 1 System Configuration With One Dominant Nonlinearity

In order to investigate LC conditions, the nonlinearity is treated as follows: First, we assume that the input σ is essentially sinusoidal, e.g., $\sigma = a\cos\omega t$, and thus the output is periodic. Expanding in a fourier series, we have

$$\phi(a\cos\omega t) = \sum_{k=1}^{\infty} \mathrm{Re}\,[b_k\,(a)\,\exp\,(jk\omega t)] \qquad (2)$$

By omitting the constant or D.C. term from Eq. (2) we are implicitly assuming that $\phi(\sigma)$ is an odd function, $\phi(-\sigma) = -\phi(\sigma)$ for all σ, so that no rectification occurs; cases when ϕ is not odd present no difficulty [1,2], but are omitted to simplify the discussion. Then we make the approximation

$$\phi(a\cos\omega t) \cong \mathrm{Re}\,[b_1\,(a)\,\exp\,(j\omega t)]$$
$$\triangleq \mathrm{Re}\,[k_1\,(a) * a\,\exp\,(j\omega t)] \qquad (3)$$

This approximate representation for $\phi\,(a\cos\omega t)$ includes only the first term of the fourier expansion of Eq. (2); therefore the approximation error is minimized in the mean square error sense [1-3]. The fourier coefficient b_1 (and thus the

"gain" k_1) is generally complex unless $\phi(\sigma)$ is single valued; the real and imaginary parts of b_1 represent the in-phase (cosine) and quadrature (-sine) fundamental components of $\phi(a \cos \omega t)$, respectively. The so-called describing function $k_1(a)$ in (3) is "amplitude dependent", thus retaining a basic property of a nonlinear operation.

By the principle of harmonic balance, the assumed oscillation -- if it is to exist -- must result in a quasi-linearized system with pure imaginary eigenvalues; substituting $\phi(\sigma) \tilde{=} k_1(a)\, \sigma$ in Eq. (1) yields

$$|j\omega \underline{\underline{I}} - \underline{\underline{F}} + k_1(a)\, \underline{g}\underline{h}^T| = 0$$

for some value of ω, or by elementary matrix operations

$$W(j\omega) = -1/k_1(a) \tag{4}$$

Condition (4) is easy to verify using the polar or Nyquist plot of $W(j\omega)$ [1,2]; in addition the LC amplitude a is determined in the process.

It is generally well-understood that the classical SIDF analysis as outlined above is only approximate, so caution is always recommended in its use. The standard caveats that $W(j\omega)$ should be "low pass to attenuate higher harmonics" and that $\phi(\sigma)$ should be "well-behaved" (so that the first harmonic in (2) is dominant) indicate that the analyst has to be cautious.

The utility of SIDF analysis for systems with one significant SISO nonlinearity as outlined above has naturally resulted in a number of attempts to generalize the technique to the multiple-nonlinearity case. In the work that preceded [4], only SISO nonlinearities were considered, and bias effects (either due to constant inputs or to "rectification" caused by nonlinear effects) were excluded. Also special model configurations were often assumed [2]. The earlier results are discussed more fully in [7]. The LC analysis approach described in this chapter and in [3] removes all restrictions with respect to model configuration, nonlinearity type, or the presence of biases.

2. THE GENERAL SIDF LIMIT CYCLE ANALYSIS METHOD

The most general system model considered here is

$$\dot{\underline{x}} = \underline{f}\,(\underline{x},\underline{u}) \tag{5}$$

when $\underline{x}$ is an n-dimensional state vector and $\underline{u}$ is an m-dimensional input vector. Assuming that $\underline{u}$ is a vector of constants, denoted $\underline{u}_o$, it is desired to determine if Eq. (5) may exhibit LC behavior.

As before, we assume that the state variables are nearly sinusoidal,

$$\underline{x} \tilde{=} \underline{x}_c + \mathrm{Re}[(\underline{a} \exp(j\omega t)] \tag{6}$$

where $\underline{a}$ is a complex amplitude vector and $\underline{x}_c$ is the state vector center value (which is not a singularity, or solution to $\underline{f}\,(\underline{x}_o, \underline{u}_o) = \underline{0}$ unless the nonlinearities satisfy certain stringent symmetry conditions with respect to $\underline{x}_o$). Then we again neglect higher harmonics, to make the approximation

$$\underline{f}(\underline{x},\underline{u}_o) = \underline{f}_{DF}(\underline{x}_c,\underline{a},\underline{u}_o) + \mathrm{Re}[\underline{\underline{F}}_{DF}(\underline{x}_c,\underline{a},\underline{u}_o)\, \underline{a} \exp(j\omega t)] \tag{7}$$

The real vector $\underline{f}_{DF}$ and the matrix $\overline{\underline{F}}_{DF}$ are obtained by taking the fourier expansions of the elements of $\underline{f}(\underline{x}_c + \text{Re } \underline{a} \exp(j\omega t), \underline{u}_o)$ as illustrated below, and provide the quasi-linear or describing function representation of the nonlinear dynamic relation. The assumed limit cycle exists for $\underline{u} = \underline{u}_o$ if $\underline{x}_c$ and $\underline{a}$ can be found so that

$$\begin{aligned} &\text{(i)} \quad \underline{f}_{DF}(\underline{x}_c, \underline{a}, \underline{u}_o) = 0 \\ &\text{(ii)} \quad [j\omega\overline{\underline{I}} - \overline{\underline{F}}_{DF}(\underline{x}_c, \underline{a}, \underline{u}_o)]\underline{a} = 0, \ \underline{a} \neq \underline{0} \end{aligned} \tag{8}$$

($\overline{\underline{F}}_{DF}$ has a pair of pure imaginary eigenvalues, and $\underline{a}$ is the corresponding eigenvector.)

The nonlinear algebraic equations (8) are often difficult to solve. A second-order DE with two nonlinearities (from a two-mode panel flutter model [8,9]) can be treated easily by direct analysis [5], as shown below. An iterative method, based on successive approximation, can be used successfully for more complicated problems such as the aircraft problem described later in this chapter.

3. APPLICATIONS

3.1 A PANEL FLUTTER PROBLEM

The following second-order differential equation has been derived to describe the local behavior of solutions to a two-mode panel flutter model [8,9]:

$$\ddot{x} + (\alpha + x^2)\,\dot{x} + (\beta + x^2)\,x = 0 \tag{9}$$

Heuristically, it is reasonable to predict that limit cycles may occur for α negative (so that damping is negative for small values of x but positive for large values). Observe also that there are three singularities if β is negative: $x_o = 0, \pm\sqrt{-\beta}$. The corresponding state vector DE is

$$\dot{\underline{x}} = \begin{bmatrix} \dot{x} \\ \ddot{x} \end{bmatrix} = \begin{bmatrix} 0 & 1 \\ -\beta & -\alpha \end{bmatrix} \underline{x} - \begin{bmatrix} 0 \\ x_1^2(x_1 + x_2) \end{bmatrix} \tag{10}$$

The SIDF assumption for this system of equations is that

$$x_1 = x = x_c + a_1 \cos \omega t$$

$$x_2 = \dot{x} = -a_1 \omega \sin \omega t$$

(From the relation $x_2 = \dot{x}_1$, it is clear that x_2 has no center value, and that $a_2 = j\omega a_1$ in (6)). Therefore, the combined nonlinearity in Eq. (10) is quasi-linearized to be

$$\begin{aligned} x_1^2(x_1 + x_2) &= (x_c + a_1 \cos \omega t)^2 \, (x_c + a_1 \cos \omega t - a_1 \omega \sin \omega t) \\ &\cong (x_c^3 + \tfrac{3}{2} a_1^2 x_c) + (3x_c^2 + \tfrac{3}{4} a_1^2)\, a_1 \cos \omega t \\ &\qquad + (x_c^2 + \tfrac{1}{4} a_1^2)(-a_1 \omega \sin \omega t) \end{aligned} \tag{11}$$

This result is obtained by expanding the first expression using trigonometric identities to reduce $\cos^2 u$, $\cos^3 u$ and $\sin u \cos^2 u$ into terms involving $\cos ku$,

sin ku, k = 0,1,2,3 and discarding all terms except the fundamental ones (k = 0,1). Therefore, the conditions of (8) require that

$$\underline{f}_{DF} = \begin{bmatrix} 0 \\ -x_c\ (\beta + x_c^2 + \frac{3}{2} a_1^2) \end{bmatrix} = \underline{0} \tag{12}$$

$$\underline{\bar{F}}_{DF} = \begin{bmatrix} 0 & 1 \\ -(\beta + 3x_c^2 + \frac{3}{4} a_1^2) - (\alpha + x_c^2 + \frac{1}{4} a_1^2) & \end{bmatrix} = \begin{bmatrix} 0 & 1 \\ -\omega^2 & 0 \end{bmatrix} \tag{13}$$

Relation (12) shows two possibilities:

$$\underline{\text{Case 1}}: \quad x_c = 0 \qquad \text{yields} \qquad \begin{aligned} a_1 &= 2\sqrt{-\alpha} \\ \omega &= \sqrt{\beta - 3\alpha} \end{aligned} \tag{14}$$

The amplitude a, and frequency ω must be real. Thus, as predicted, $\alpha < 0$ is required for an LC to exist centered about the origin. The second parameter must satisfy $\beta > 3\alpha$, so β can take on any positive value but cannot be more negative than 3α.

$$\underline{\text{Case 2}}: \quad x_c = \pm \sqrt{\frac{\beta - 6\alpha}{5}} \qquad \text{yields} \qquad \begin{aligned} a_1 &= 2\sqrt{\frac{\alpha - \beta}{5}} \\ \omega &= \sqrt{\beta - 3\alpha} \end{aligned} \tag{15}$$

For the two case 2 limit cycles to exist, it is necessary that $3\alpha < \beta < \alpha$, so again limit cycles cannot exist unless $\alpha < 0$. Two additional constraints must be imposed: $|x_c| > a_1$ must hold or the two limit cycles will overlap; this condition reduces the permitted range of β to $2\alpha < \beta < \alpha$. Also, for $2\alpha < \beta < \alpha$ the case 2 LC's must lie inside the case 1 LC which also exists for this range of β; from Eqs. (14) and (15) this is indeed satisfied over the range $2\alpha < \beta < \alpha$.

The stability of the case 1 LC can be determined as follows: Take any $\varepsilon > 0$ and let $a_1^2 = -4\alpha - \varepsilon < -4\alpha$; then $\underline{\bar{F}}_{DF}$ is

$$\underline{\bar{F}}_{DF} = \begin{bmatrix} 0 & 1 \\ -(\beta - 3\alpha - \frac{3}{4}\varepsilon) & \frac{1}{4}\varepsilon \end{bmatrix}$$

which for $\varepsilon > 0$ has slightly unstable eigenvalues. Thus a trajectory just inside the LC will grow, indicating that the case 1 LC is stable. A similar analysis of the case 2 LC is more complicated, and thus omitted.

Another viewpoint is provided by the traditional singularity analysis approach (refer to [10]), which involves linearization about $x = 0$ and (if $\beta < 0$) $x = \pm \sqrt{-\beta}$. The linearized $\underline{\bar{F}}$-matrices and singularity characterizations for $\alpha < 0$ are given as follows:

$$\underline{x = 0}: \quad \underline{\underline{F}} = \begin{bmatrix} 0 & 1 \\ -\beta & -\alpha \end{bmatrix} \begin{cases} \beta < 0 \rightarrow \text{saddle} \\ 0 < \beta < \frac{1}{4}\alpha^2 \rightarrow \text{unstable node} \\ \beta > \frac{1}{4}\alpha^2 \rightarrow \text{unstable focus} \end{cases}$$

$$\underline{x = \pm \sqrt{-\beta}}: \quad \underline{\underline{F}} = \begin{bmatrix} 0 & 1 \\ 2\beta & \beta-\alpha \end{bmatrix} \begin{cases} \beta_1 < \beta < 0 \rightarrow \text{unstable node} \\ \alpha < \beta < \beta_1 \rightarrow \text{unstable focus} \\ \beta = \alpha \rightarrow \text{center} \\ \beta_2 < \beta < \alpha \rightarrow \text{stable focus} \\ \beta < \beta_2 \rightarrow \text{stable node} \end{cases}$$

where

$$\beta_1 = (\alpha - 4) + 2\sqrt{4 - 2\alpha}$$

$$\beta_2 = (\alpha - 4) - 2\sqrt{4 - 2\alpha}$$

The LC analysis and singularity analysis are completely consistent for $\alpha < 0$, $\beta > 2\alpha$. For all $\beta > 0$, the single singularity is unstable, and for $\alpha < \beta < 0$, the three singularities are unstable, so in both cases the predicted existence of a single stable LC is reasonable. For $\beta = \alpha$, the existence of two center singularities at $x_o = \pm \sqrt{-\beta}$ is in exact accordance with the condition $\beta < \alpha$ for two interior limit cycles to exist, with centers $x_c \cong \pm \sqrt{-\beta}$. The only range of β which seems to give rise to contradictory results is $3\alpha < \beta < 2\alpha$, where the disappearance of the two inner LC's is not consistent with the stable nature of the singularities at $x_o = \pm \sqrt{-\beta}$ and the continuing presence of a large stable LC centered about the origin. The seemingly anomalous result that the SIDF analysis predicts the existence of two overlapping LC's for $3\alpha < \beta < 2\alpha$ might suggest that there may in fact be a single "peanut-shaped" LC inside the large stable LC -- but such a conclusion would only be an intuitive speculation. Since the conjectured inner limit cycle would be quite distinctly nonsinusoidal, it would be necessary to include higher harmonics (e.g., $\underline{x} = \underline{x}_c + \text{Re}\,[\underline{a}_1 \exp j\omega t)] + \text{Re}\,[\underline{a}_3 \exp (3j\omega t)]$) in the SIDF analysis in order to reveal its presence. Such an assumption gives rise to substantially more complicated LC existence conditions, so it is not pursued here.

In the terminology of bifurcation theory, we observe that the SIDF analysis indicates the following:

- Bifurcation from a single stable singularity at $x = 0$ to a single stable LC centered about $x = 0$ for $\beta > 0$, α passing from positive to negative,
- Bifurcation from one stable LC enclosing three unstable singularities to one stable LC enclosing two unstable LC's and a saddle for $\alpha < 0$, β passing from greater than α to less than α,

- Disappearance of the two inner LC's for $\alpha < 0$, $\beta < 2\alpha$,
- Disappearance of all limit cycles for $\beta < 3\alpha$.

One quite simple analysis has revealed a great deal of the rich variety of behavior that the DE can exhibit, as illustrated in Fig. 2.

3.2 A HIGHLY NONLINEAR AIRCRAFT DYNAMICS MODEL

In a realistic model of the dynamics of a high-performance aircraft at moderate angle of attack, one is confronted with a large number of nonlinearities. These nonlinearities arise from the empirical aerodynamic data for the specific aircraft (aerodynamic coefficients and stability derivatives) and from dynamic and kinematic effects. The state equations for the aircraft motion can be written in body axes as in Eq. (16) if small off-diagonal moment-of-inertia terms and nonaxial thrust components are neglected [11]:

$$\dot{\underline{x}} \triangleq \begin{bmatrix} \dot{\theta} \\ \dot{u} \\ \dot{q} \\ \dot{w} \\ \dot{v} \\ \dot{r} \\ \dot{p} \\ \dot{\phi} \end{bmatrix} = \begin{bmatrix} q\cos\phi - r\sin\phi \\ (X+T)/m + rv - qw - g\sin\theta \\ ((I_z - I_x)pr + M)/I_y \\ Z/m + qu - pv + g\cos\phi\cos\theta \\ Y/m + pw - ru + g\sin\phi\cos\theta \\ ((I_x - I_y)pq + N)/I_z \\ ((I_y - I_z)qr + L)/I_x \\ p + q\sin\phi\tan\theta + r\cos\phi\tan\theta \end{bmatrix} \triangleq \underline{f}(\underline{x},\underline{u}) \qquad (16)$$

The state variables are the aircraft velocity components in body axes (u,v,w), the rotational rates about the body axes (p,q,r), and the pitch and roll Euler angles (θ,ϕ). The parameters g, m, I_x, I_y, I_z denote the acceleration due to gravity and the aircraft mass and moments of inertia, respectively.

The aircraft data and response characteristics are associated with the force and moment components, X, Y, Z, L, M, N; these contributions are expressed in terms of non-dimensional aerodynamic force and moment coefficients, for example,

$$L = \frac{1}{2}\rho V^2 S b C_{\ell_T} \qquad (17)$$

where ρ represents air density, V is the velocity vector magnitude, and S and b denote reference area and wing span. The aerodynamic coefficients are determined by the aircraft control settings,

$$\underline{u}^T = [\delta_s \ \delta_{sp} \ \delta_{ds} \ \delta_r]$$

which are stabilator, spoiler, differential stabilator and rudder, respectively. In addition, they are highly nonlinear functions of angle of attack and sideslip angle,

$$\alpha = \tan^{-1}(w/u) \qquad \beta = \sin^{-1}(v/V)$$

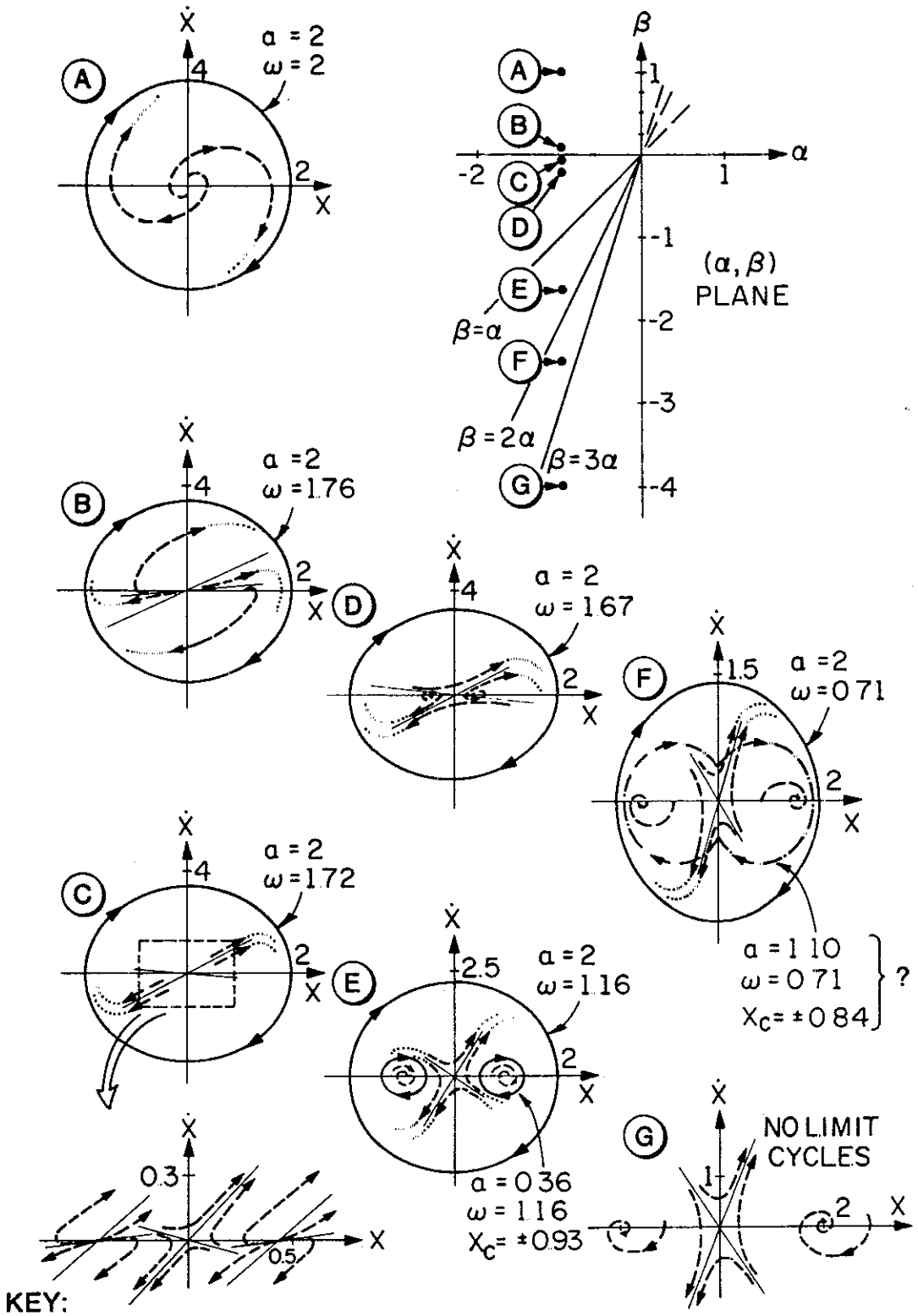

Fig. 2 Qualitative Behavior of the Panel Flutter Model

In terms of these variables, the force and moment contributions as in Eq. (17) are represented in standard form; for example,

$$C_{\ell_T} = C_\ell(\alpha,\beta) + C_{\ell_{\delta_{ds}}}(\alpha)\delta_{ds} + C_{\ell_{\delta_{sp}}}(\alpha)\delta_{sp} + C_{\ell_{\delta_r}}(\alpha)\delta_r + \frac{b}{2V}\left[C_{\ell_r}(\alpha)r + C_{\ell_p}(\alpha)p\right] \tag{18}$$

The nonlinear terms in Eq. (18) were supplied in the form of empirically determined values of the aerodynamic coefficients and stability derivatives at various flight conditions. Based on this information, analytic representations were developed by curve fitting; for example,

$$C_{\ell_p} = -k_{34}(1 + k_{35}\,\alpha + k_{36}\,\alpha^2) \tag{19}$$

Finally, the approximations

$$V = \sqrt{u^2+v^2+w^2} \cong u$$

$$\alpha = \tan^{-1}(w/u) \cong w/u$$

$$\beta = \sin^{-1}(v/V) \cong v/u$$

are used in most instances. The resulting highly nonlinear model with k_i suitably evaluated in the curve fit relations as in Eq. (19) is realistic for the aircraft considered at angles of attack between 15 and 30 deg.

The nonlinearities in Eq. (16) which were selected for rigorous study are $(-r \sin \phi)$, $(I_z - I_x)pr$, Z, N, and L. These five terms are potentially important in studying lateral-mode oscillations, including possible "wing rock" mechanisms, so they were quasi-linearized; the remaining terms in Eq. (16) were handled by small-signal linearization.

Before LC analysis is undertaken, it is useful to obtain the complete equilibrium or trim condition, i.e., the values of $\underline{x}_0$ and $\underline{u}_0$ that satisfy

$$\underline{f}(\underline{x}_0, \underline{u}_0) = \underline{0} \tag{20}$$

determined according to Eq. (16). In a preliminary investigation of aircraft behavior for various flight regimes, complete small-signal linearization is useful; the $(n \times n)$ matrix $\overline{\underline{F}}_0$ defined by

$$\overline{\underline{F}}_0 \triangleq \frac{\partial \underline{f}}{\partial \underline{x}}\bigg|_{\underline{x}=\underline{x}_0,\ \underline{u}=\underline{u}_0} \tag{21}$$

determines the dynamic properties of the perturbation equation corresponding to Eq. (16). The small-signal eigenvalues, or solutions $\lambda_{0,k}$, $k = 1, 2, \ldots, n$, to the characteristic equation

$$\det(\lambda_0 \overline{\underline{I}} - \overline{\underline{F}}_0) = 0 \tag{22}$$

govern the transient response of the aircraft to small perturbations for a fixed control setting $\underline{u}(t) \equiv \underline{u}_0$.

For small α, the eigenvalues given by small-signal linearization are generally moderately well damped, and nonlinear effects may not be important. As α increases damping generally decreases, so the nonlinear effects become critical in determining the behavior of the aircraft, and LC conditions may exist.

The iterative solution of condition (8) proceeds as follows: First, assume that an oscillation exists in the system. For the present problem, it is natural to assume that the steady-state angle of attack satisfies

$$\alpha = \alpha_0(1 + \kappa \sin \omega t) \tag{23}$$

where α_0 is moderate and κ is generally less than unity[1]. The assumed frequency, ω, is initially the imaginary part of the most lightly damped eigenvalue given by small-signal linearization; ω will be adjusted in the subsequent iterations. The goal of the limit cycle investigation is to determine either that some κ (or several values of κ) exists such that Eq. (23) is a valid assumption (limit cycles are predicted), or that no value κ can be found for which Eq. (23) is consistent with condition (8) (limit cycles probably are not present). The LC analysis computer program developed for such a determination uses the method of successive approximation, and is doubly iterative, as follows:

Step 0: Set i=0; start the procedure with $\underline{x}_{c,i} = \underline{x}_0$ satisfying Eq. (20) and $\overline{\underline{F}}_{DF,i} = \overline{\underline{F}}_0$ from Eq. (21).

Step 1: Choose a trial value of κ in Eq. (23), e.g., $\kappa = 0.1$.

Step 2: Based on the assumed oscillation, Eq. (23), and the current quasi-linear system dynamics matrix $\overline{\underline{F}}_{DF,i}$, determine the amplitudes of oscillation throughout the system model by finding $\underline{a}_i$ in the steady-state solution

$$\underline{x} = \underline{x}_{c,i} + \text{Re}\ (\underline{a}_i \exp(j\omega t)) \tag{24}$$

Step 3: Using the quasi-linear system model, Eq. (7), determine the adjusted center $\underline{x}_{c,i+1}$ satisfying

$$\underline{f}_{DF,i}(\underline{x}_{c,i+1}, \underline{a}_i, \underline{u}_0) = \underline{0} \tag{25}$$

which reflects the change in $\underline{x}_c$ caused by the postulated sinusoidal component of $\underline{x}$.

Step 4: Obtain the adjusted quasi-linear system dynamics matrix $\overline{\underline{F}}_{DF,i+1}$ $(\underline{x}_{c,i+1}, \underline{a}_i, \underline{u}_0)$ which contains the sinusoidal-component describing function gains for all nonlinearities. Reset i = i+1.

Step 5: Calculate the adjusted frequency, ω_i, which is the imaginary part of the most lightly damped of the quasi-linear eigenvalues of $\overline{\underline{F}}_{DF,i}$.

Step 6: Check to see if the iterative center determination procedure has converged; if not, return to Step 2; if so, continue to Step 7.

Step 7: Compare the most lightly-damped eigenvalues with those obtained for

---

[1] Choosing the sinusoidal component amplitude to be $\kappa\alpha_0$ often leads to a convenient normalization. For limit cycle analysis about a zero center value, it would not be appropriate.

the previous trial value of κ, denoted $\bar{\kappa}$ (in the first trial $\bar{\kappa} = 0$, i.e., the eigenvalues are as obtained by small-signal linearization, Eq. (22)):

- If the pair of eigenvalues near the imaginary axis has crossed the axis, then some value of κ exists in the range $(\bar{\kappa}, \kappa)$ such that one pair of the adjusted quasi-linear eigenvalues $\lambda_{i,k}(\kappa)$ is on the imaginary axis -- a limit cycle is predicted. The value of κ, denoted κ_0, can be found by further iteration on κ.
- If the pair of eigenvalues near the imaginary axis remains on the same side of the axis, increment κ (for example, by adding $\Delta\kappa = 0.1$) and repeat Steps 2 to 7.

Steps 2 to 6 represent an iterative solution of the steady-state conditions for the bias component or "center" of the assumed oscillation; condition (8(i)) is thereby satisfied. The term center is used to distinguish $\underline{x}_c$ from the equilibrium $\underline{x}_0$ satisfying Eq. (20). Step 7 is a test to see if condition (8(ii)) can be met for some κ.

If for a representative set of values of κ (e.g., $\kappa = 0, 0.1, 0.2, \ldots, 2.0$) the most lightly damped eigenvalue pair does not cross the imaginary axis, then it is predicted that limit cycles cannot exist for the particular fixed control setting $\underline{u}_0$. Otherwise, the above procedure will iterate to find the value or values of κ which corresponds to probable limit cycle amplitudes.

One detail regarding the procedure mentioned in Step 2 is in order, since it is central to this technique. Given the quasi-linear system dynamics matrix that is known from the previous iteration, $\bar{\underline{F}}_{DF,i}$, plus an assumed oscillation in one state,

$$x_k = a_k \cos(\omega_i t)$$

(neglecting the bias component for simplicity), it is desired to determine the complex vector of amplitudes, $\underline{a}$, such that $\underline{x} = \mathrm{Re}\,[\underline{a} \exp(j\omega_i t)]$. If ω_1 is a natural frequency corresponding to $\dot{\underline{x}} = \bar{\underline{F}}_{DF,i}\underline{x}$, then (cf. condition (8))

$$(j\omega_i \bar{\underline{I}} - \bar{\underline{F}}_{DF,i})\underline{a} = \underline{0} \tag{26}$$

The latter relation serves to define the entire vector $\underline{a}$, given one of its elements, a_k, by deleting one of the equations in Eq. (26) and solving the remaining (n-1) equations. The solution $\underline{a}$ for specified a_k is not unique unless ω_i is actually an eigenvalue of $\bar{\underline{F}}_{DF,i}$; this will be true only for a value of κ for which limit cycles are predicted. This approach is dealt with in more detail in [6,7].

The aerodynamic data curve fits obtained by adjusting the coefficients k_i as in Eq. (19) were initially verified by determining the eigenvalues obtained by small-signal linearization, for various trim values of angle of attack. Good agreement with the empirical aero model was obtained; in particular, the Dutch roll mode stability boundary given by small-signal linearization of the curve fit model agreed with that given by the experimental aerodynamic model which showed

marginal stability for $\alpha \cong 19.6$ deg. This case ($\alpha = 19.6$ deg) corresponds to the nearly straight-and-level flight condition specified in Table 1; the corresponding control setting $\underline{u}_0$ was therefore chosen for study since small-signal linearization leads to nearly marginal stability and higher-order nonlinear terms thus become critical in determining the aircraft performance. The corresponding eigenvalues associated with the Dutch roll mode are $\lambda_{DR} = 0.0366 \pm 1.52j$, which for small perturbations predicts an unstable response. It is important to note that there is a much slower unstable lateral mode ("lateral phugoid"), with eigenvalues $\lambda_{LP} = 0.0187 \pm 0.131j$. In most instances, a mode which is as slow as the lateral phugoid in the present case is not a concern, so attention is generally restricted hereafter to the behavior of the Dutch roll mode.

Table 1. Selected Equilibrium Condition

STATE VARIABLE (ELEMENT OF $\underline{x}_0$)	VALUE
θ_0	17.46 deg
u_0	81.7 m/sec
q_0	0.296 deg/sec
w_0	29.1 m/sec
v_0	6.04 m/sec
r_0	-0.033 deg/sec
p_0	-0.011 deg/sec
ϕ_0	-5.303 deg

The multivariable LC analysis computer program described above was then used to find limit cycle conditions. It was found that λ_{DR} is virtually on the imaginary axis, $\lambda_{DR} = 4\times10^{-5} \pm 1.495j$ for κ equal to 1.20. Corresponding to this value of κ, the "center" value $\underline{x}_c$ and oscillation component $\underline{a}$ for the state vector are given in Table 2.

Table 2. Center and Predicted Limit Cycle Amplitude for the Stable Limit Cycle

STATE VARIABLE CENTER (ELEMENT OF $\underline{x}_c$)		Re($\underline{a}$)	Im($\underline{a}$)	UNITS
θ_c	18.35	0.259	-0.234	deg
u_c	80.25	-0.177	0.165	m/sec
q_c	0.174	0.219	0.182	deg/sec
w_c	28.80	-0.810	-0.718	m/sec
v_c	6.14	7.38	0.0	m/sec
r_c	0.792	-1.79	-1.89	deg/sec
p_c	-0.310	-7.35	14.90	deg/sec
ϕ_c	8.55	9.55	5.295	deg

Checking the limit cycle prediction requires that nonlinear simulations of the dynamics specified in Eqs. (16-19) be performed. Choice of the initial condition for this procedure is critical, because there also exists an unstable mode, a slow spiral mode which for $\kappa = 1.2$ is governed by $\lambda_s = 0.0618$. If this mode is excited appreciably, its growth will completely obscure the fast limit cycle that is sought. Fortunately, choosing $\underline{x}(0) \propto \text{Re } \underline{a}$ will make the limit cycle in the Dutch roll mode be the dominant mode.

This limit cycle prediction shown in Table 2 was checked by choosing $x(0) = 0.8 \text{ Re } a$. The resulting time histories of pitch angle θ,y body-axis

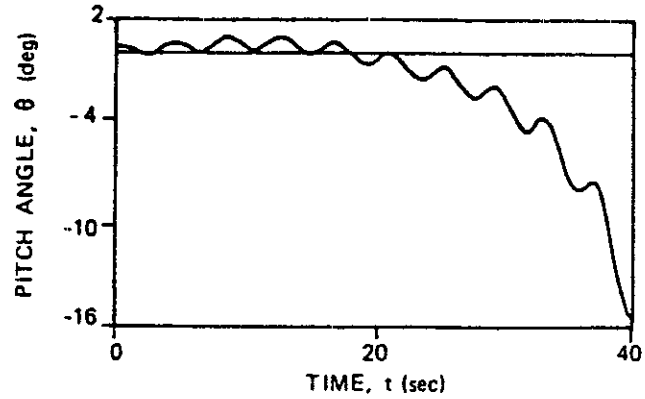

(a) PITCH ANGLE TIME HISTORY

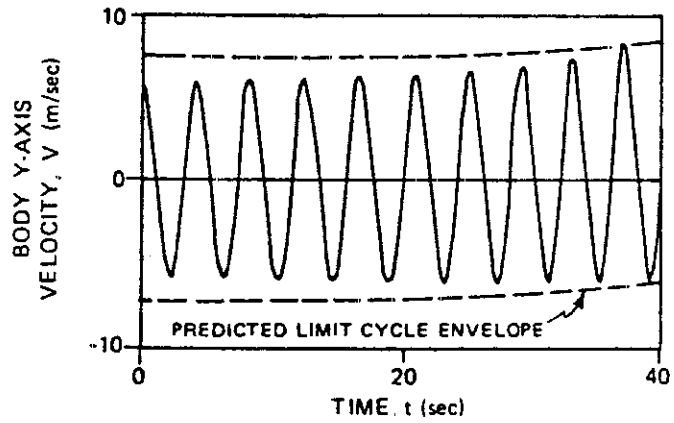

(b) BODY Y-AXIS VELOCITY TIME HISTORY

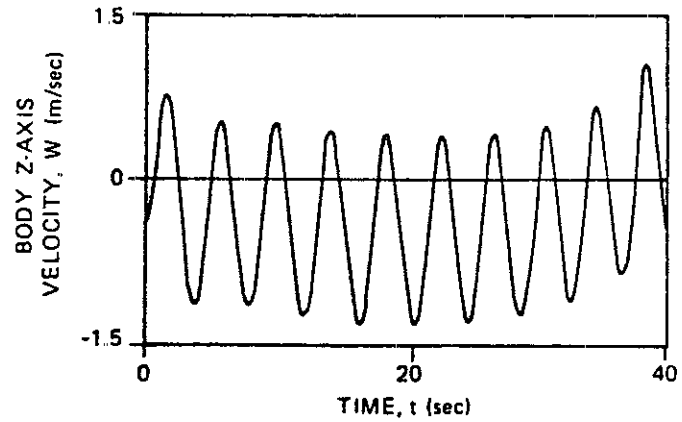

(c) BODY Z-AXIS VELOCITY TIME HISTORY

Fig. 3 Simulation of the Limit Cycle Prediction

velocity v, and z body-axis velocity w, are portrayed[2] in Fig. 3. The plot of θ shows that the solutions do diverge very slowly, due to a small unavoidable excitation of the spiral mode. The time histories of v and w show that the dominant Dutch roll mode is very slowly growing for the first 25 sec of the simulation, as would be expected for an initial condition that is slightly interior to the predicted limit cycle. The predicted center value of v is nearly exact, while that for w is in error by about -0.5 m/sec, or about -1.7 percent. Finally, the predicted limit cycle frequency is 1.495 rad/sec, while the observed frequency is 1.497 rad/sec; the agreement is excellent. After 25 sec of simulation, the slow divergence begins to alter the limit cycle that developed in the first part.

Further analysis of the simulation results was undertaken to attempt to separate out the effect of the slow divergence. The time history depicted in Fig. 3b was processed to determine the exponential growth component ($c_1 e^{c_2 t}$); then the predicted limit cycle envelope is given by the relation

$$E_{LC} = c_1 e^{c_2 t} \pm |a_5|$$

where $|a_5|$ is the amplitude of the predicted limit cycle in v (state 5). This envelope is portrayed in Fig. 3b; within the limits of the simulation accuracy, convergence of the time history to the envelope is shown.

The effort to verify the limit cycle condition by direct simulation has pointed up a major difficulty in using the latter technique as an exploratory tool to locate limit cycles, without recourse to describing function analysis. Realistic aerodynamic models such as those used here often have slow modes that are unstable or that are very lightly damped. Initial conditions for direct simulation must be chosen very carefully to avoid exciting these modes. In a linear system, it is not difficult to use eigenvector information to obtain initial conditions that selectively excite a desired mode. However, eigenvectors are not rigorously defined for nonlinear systems.

The concept which was successfully used in this study may be called the quasi-linear eigenvector; in essence, the complex vector $\underline{a}$, given as in Table 2, is in a sense an amplitude-specific eigenvector, which specifies an initial condition that only excites the predicted oscillation. The fact that the quasi-linear eigenvector $\underline{a}$ is amplitude-dependent is illustrated in Fig. 4, which shows $\underline{a}$ for three values of κ, corresponding to the study depicted in Fig. 3. For $\kappa = 1.0$ and 1.5, the eigenvector components for θ and q are too small to be shown; the differences between the remaining components (which are normalized to make the length of the v component equal in each plot) are rather small. For $\kappa = 2.5$, the changes in $\underline{a}$ are clearly quite substantial.

---

[2] The plots show the perturbation of each variable about the predicted center value, x_c, Table 2.

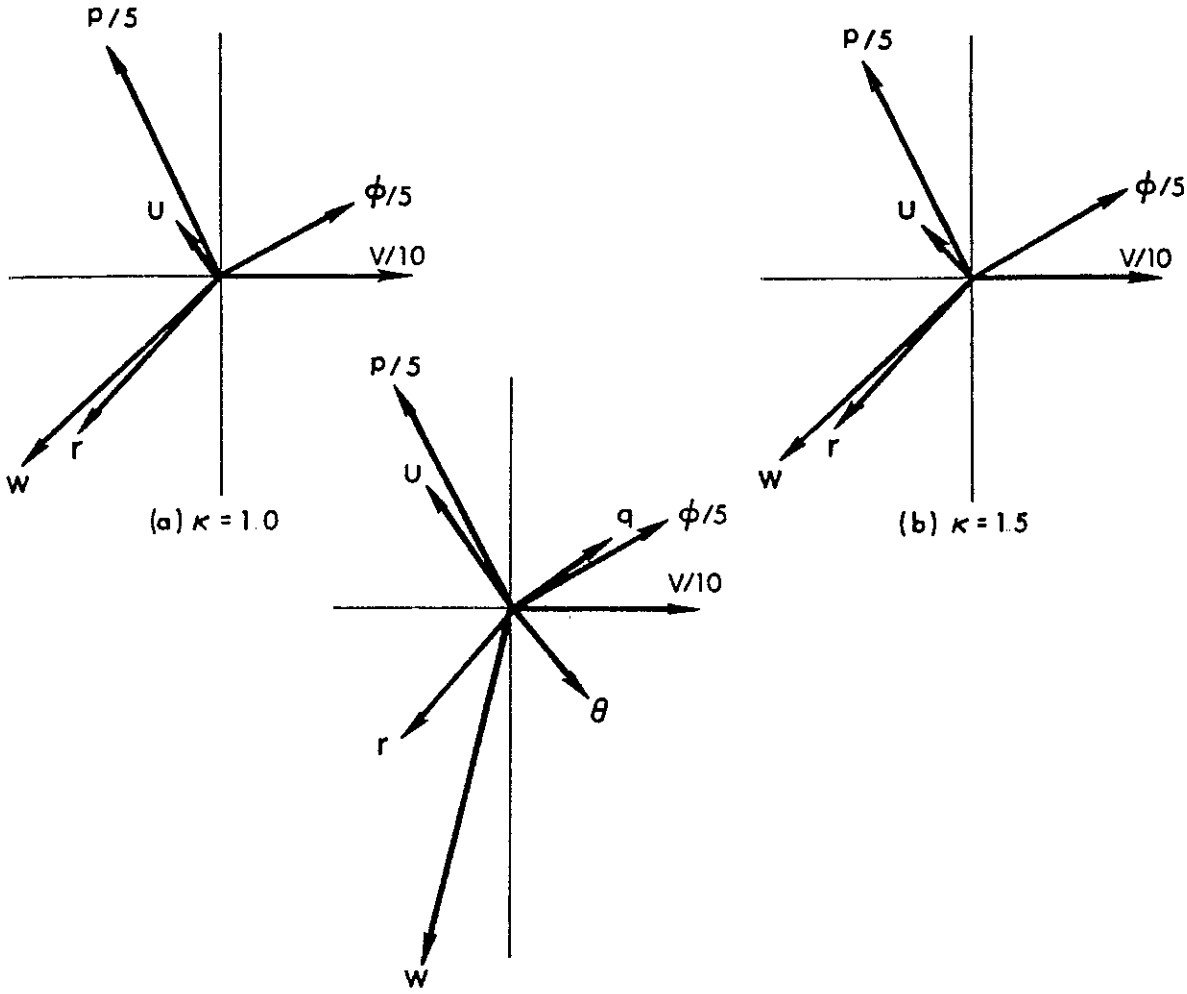

Fig. 4 Amplitude-Dependent Quasi-linear Eigenvectors[3]

4. SUMMARY AND CONCLUSIONS

The SIDF technique described in this chapter and in [3] permits the investigation of LC conditions in completely general multivariable nonlinear systems. Restrictions as to the type and number of nonlinearities, the system configuration and the presence of constant inputs have been completely removed.

The studies presented here illustrate the effectiveness of the general LC analysis method. The predicted LC frequency and center value (Fig. 3) are in good agreement with the simulation results; the accuracy of the amplitude prediction is more difficult to assess quantitatively due to the simulation problems mentioned previously (see Fig. 3b). In general, these results bolster the expectation that the iterative LC analysis technique will be found to converge to locate limit cycle conditions, provided that limit cycles indeed exist. Considerable further research could be performed to conclusively demonstrate the power and accuracy of the general SIDF LC analysis approach, and its limitations.

A major point of departure from previous SIDF analysis methods is the sub-

[3] The eigenvectors correspond to θ, u, q, w, v/10, r, p/5, φ/5; this scaling was performed to permit all components of $\underline{a}$ to be shown on the plots for κ = 2.5.

stitution of root locus-like plots of quasi-linear eigenvalues, e.g., the locus of λ_{DR} for various values of K, in lieu of frequency-response plots based on $W(j\omega)$ and $-1/k_1(a)$. This alternative viewpoint has permitted the breakthrough in terms of system model generality in comparison with frequency-domain SIDF techniques for multivariable systems. As a result, one loses the ability to modify or remove LC conditions by the classical methods for altering the frequency response of $W(s)$ by changing pole locations or adding compensation networks. However, systems designers versed in the more modern technique of pole placement using state variable feedback should find that method of system response compensation applicable to LC conditions found using this new SIDF technique; an approach due to Sankaran [12] appears to be particularly useful in this regard. Combining the general SIDF LC analysis method with an iterative pole position modifying algorithm would result in a very powerful approach to multivariable nonlinear systems synthesis.

Finally, other benefits of this technique are

- Any number of nonlinear effects can be investigated, singly or in any combination, without manipulating the system model into the "linear plant with nonlinear feedback" formulation required in the frequency-domain approach;
- An iterative algorithmic approach to limit cycle analysis is desirable for mechanization on digital computers;
- The amount of computer time required to determine the existence of limit cycles by the general SIDF approach should generally be significantly less than the computer time expenditure that would be needed using direct simulation alone as a way to search for LC conditions.

The last observation is based on the difficulty of choosing the direct simulation initial condition correctly to excite only the desired nearly oscillatory mode, as discussed in the preceding section.

Acknowledgment

The development of the general LC analysis method and the associated iterative computer program, and the aircraft performance analysis, were sponsored by the U.S. Office of Naval Research under Contract Number N00014-75-C-0432.

REFERENCES

[1] Gelb, A. and Vander Velde, W. E., Multiple-Input Describing Functions and Nonlinear System Design, McGraw-Hill, New York, 1968.

[2] Atherton, D. P., Nonlinear Control Engineering, Van Nostrand Reinhold, New York, 1975.

[3] Hedrick, J. K. and Paynter, H. M. (Eds.), Nonlinear System Analysis and Synthesis: Vol. 1 - Fundamental Principles, Chapter 4, American Society of Mechanical Engineers, New York, 1978.

[4] Taylor, J. H., "An Algorithmic State-Space/Describing Function Technique for Limit Cycle Analysis," IOM, The Analytic Sciences Corporation (TASC), Reading, Massachusetts, April 1975. (Also issued as TASC IIM-612-1 to the Office of Naval Research, Oct. 1975).

[5] Taylor, J. H., "A General Limit Cycle Analysis Method for Multivariable Systems," Engineering Foundation Conference in New Approaches to Nonlinear Problems in Dynamics, Asilomar, Calif., December 1979.

[6] Taylor, J. H., et al, "High Angle of Attack Stability and Control," Office of Naval Research Report ONR-CR215-237-1, April 1976.

[7] Taylor, J. H., "A New Algorithmic Limit Cycle Analysis Method for Multivariable Systems," TIM-612-2, TASC, Reading Massachusetts, Oct. 1977; also presented at the IFAC Symp. on Multivariable Systems, U. of New Brunswick, Fredericton, N.B. Canada, July 1977.

[8] Holmes, P. J. and Marsden, J. E., "Bifurcations to Divergence and Flutter in Flow Induced Oscillations - An Infinite Dimensional Analysis," Automatica, Vol. 14, pp. 367-384, 1978.

[9] Carr, J., Application of Center Manifold Theory, Lefchetz Center for Dynamical Systems, Div. of Appl. Math, Brown U., Providence, R.I., 1979.

[10] Cunningham, W. J., Nonlinear Analysis, McGraw-Hill, New York, 1958.

[11] Etkin, B., Dynamics of Atmospheric Flight, John Wiley, New York, 1972.

[12] Sankaran, V., "An Iterative Technique to Stabilize a Linear Constant System," IEEE Trans. on Automatic Control, Vol. AC-20, No. 2, April 1975.